Progress In Electromagnetics Research C, Vol. 71, 177–187, 2017

Compact Dual-Mode Microstrip Bandpass Filters with Transmission Zeros Using Modified Star Shaped Resonator

Kenganahalli G. Avinash and Inabathini Srinivasa Rao*

Abstract—A modified star-shaped dual-mode microstrip loop resonator with a triangular patch is proposed to design compact narrow band bandpass filters with transmission zeros. The triangular patch is used as perturbation element to couple degenerated modes. The position of transmission zeros can be tuned by varying the size and location of the perturbation element. The coupling mechanism (inductive or capacitive) and the type of input/output feed (orthogonal or non-orthogonal) determine the type of filter response like symmetric or asymmetric. Three highly selective two-pole narrow band bandpass filters are designed using a modified star-shaped resonator with tunable transmission zeros. First, two filters with non-orthogonal feed lines have an asymmetric response with transmission zeros on one side of the passband, whereas the third filter with orthogonal feed lines exhibits symmetric frequency response with transmission zeros on both sides of the passband. Even and odd mode analysis is applied to the dual-mode filters to calculate the position of transmission zeros. Filters are realized using a low loss dielectric substrate, and measured results are in good agreement with the theoretical and simulated ones.

1. INTRODUCTION

Modern wireless communication systems demand high-quality bandpass filters with features such as narrow bandwidth, high selectivity and compact size [1]. The selectivity of a bandpass filter can be improved by increasing the order of the filter, but it will increase the size of the filter and lower the insertion loss due to the increase in the number of resonators. Without increasing the order of the filter, selectivity can be improved by introducing transmission zeros on both sides of the passband. This will enhance the performance of the system and make use of the expensive spectrum effectively. Furthermore, applications such as duplexers and multiplexers require high selectivity only on one side of the passband [2]. Bandpass filters designed using resonators with dual-mode operation will improve the selectivity along with symmetric and asymmetric frequency responses. Also, the dual-mode filters are compact in size as two resonant modes are realized in single dual-mode resonator which reduces the filter size to half. Various types of dual-mode resonators have been analyzed comprising loop [3–6] and patch resonators [7–9].

In this paper, highly selective narrow bandpass filters are designed using a modified star-shaped microstrip loop resonator [10] with dual degenerate modes which employ both orthogonal and non-orthogonal feed lines. The selection of orthogonal [11–14] and non-orthogonal [15–18] feed lines used in the design of filters influences the frequency response. A small triangular patch is used as a perturbation element to couple degenerated modes. The size and shape of perturbation element will decide the frequency response of the filter like Chebyshev, elliptic or quasi-elliptic [7] as the nature of coupling will differ from one structure to another. The location of transmission zeros are calculated theoretically by applying even and odd mode analysis to the dual-mode filters. It is also shown that position of

Received 28 December 2016, Accepted 11 February 2017, Scheduled 27 February 2017
* Corresponding author: Inabathini Srinivasa Rao (israo@vit.ac.in).
The authors are with the School of Electronics Engineering, VIT University, Vellore, Tamilnadu 632014, India.

transmission zeros are tunable by shifting the position of small perturbation element. Generally, dual-mode resonators are fed by a pair of orthogonal feed lines to produce the symmetrical response, but in this paper, we use non-orthogonal feed lines, which generate asymmetrical frequency responses. This permits a simple design to fulfil the needs of uneven sideband requirements. The rest of the paper is organized as follows. Section 2 explains dual-mode properties of the proposed star-shaped loop resonator. Section 3 explains even and odd mode analysis of the filters. Asymmetric and symmetric frequency response bandpass filter designs are detailed in Section 4. Finally, conclusions are presented in Section 5.

2. DUAL-MODE STAR SHAPED RESONATOR

The proposed structure of the star-shaped single mode resonator is depicted in Fig. 1, and the structure is symmetrical along both horizontal (H-H') and vertical (V-V') planes. The input and output feed lines are not connected directly to the resonator but parallel coupled to the resonator along a straight line. The feedlines in single mode operation shown in Fig. 1 are symmetrical to both horizontal and vertical planes of the structure. Normally dual-mode filters use orthogonal feed lines to achieve symmetric frequency response which sometimes may be difficult to interface to the following circuits in a series configuration. The circumference of the modified star shaped resonator is approximately one guided wavelength. The dimensions of the filter are $a = 3\,\text{mm}$, gap $= 0.2\,\text{mm}$ and $w = 0.59\,\text{mm}$. The filters are designed on a substrate with a dielectric constant of 10.2 and thickness of 0.635 mm and the structures are simulated using a full-wave electromagnetic simulator. The frequency response of this resonator filter is shown in Fig. 2, and the filter shows single mode operation resonating at 4.14 GHz. Splitting and coupling of dual degenerate modes are essential in realizing bandpass filter using dual-mode resonators. To achieve dual-mode operation, a perturbation element in the form of a triangular patch is introduced at different symmetry planes like vertical (V-V'), horizontal (H-H')and diagonal (D-D') planes as indicated in Fig. 3(a), Fig. 3(b) and Fig. 3(c) where perturbation element will split and couple the degenerated modes. The feedlines in dual-mode operation shown in Fig. 3(a) and Fig. 3(b) are symmetrical to vertical plane of the structure whereas in Fig. 3(c) feedlines are orthogonal to each other. As mentioned before, based on size and shape of the patch the nature of coupling will change, i.e., capacitive or inductive. The size and location of perturbation element along with the position of feed lines are important in generating transmission zeros on either side of passband to have different frequency responses.

To understand the impact of perturbation element size and location on mode splitting characteristics, the resonator structures shown in Fig. 3(a) and Fig. 3(b) are simulated under weak coupling for various patch sizes and the frequency response characteristics are shown in Fig. 4(a) and

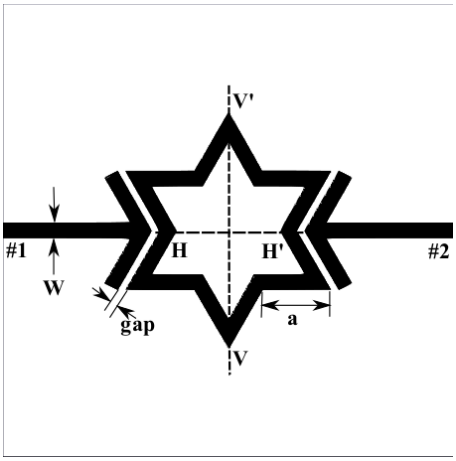

Figure 1. Proposed star-shaped loop resonator bandpass filter.

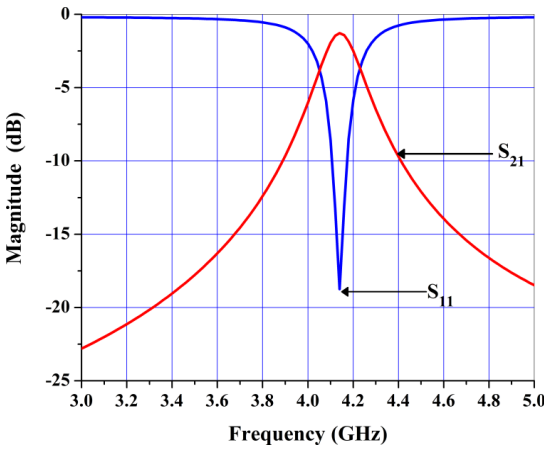

Figure 2. Insertion and return loss response of single mode star shaped loop resonator.

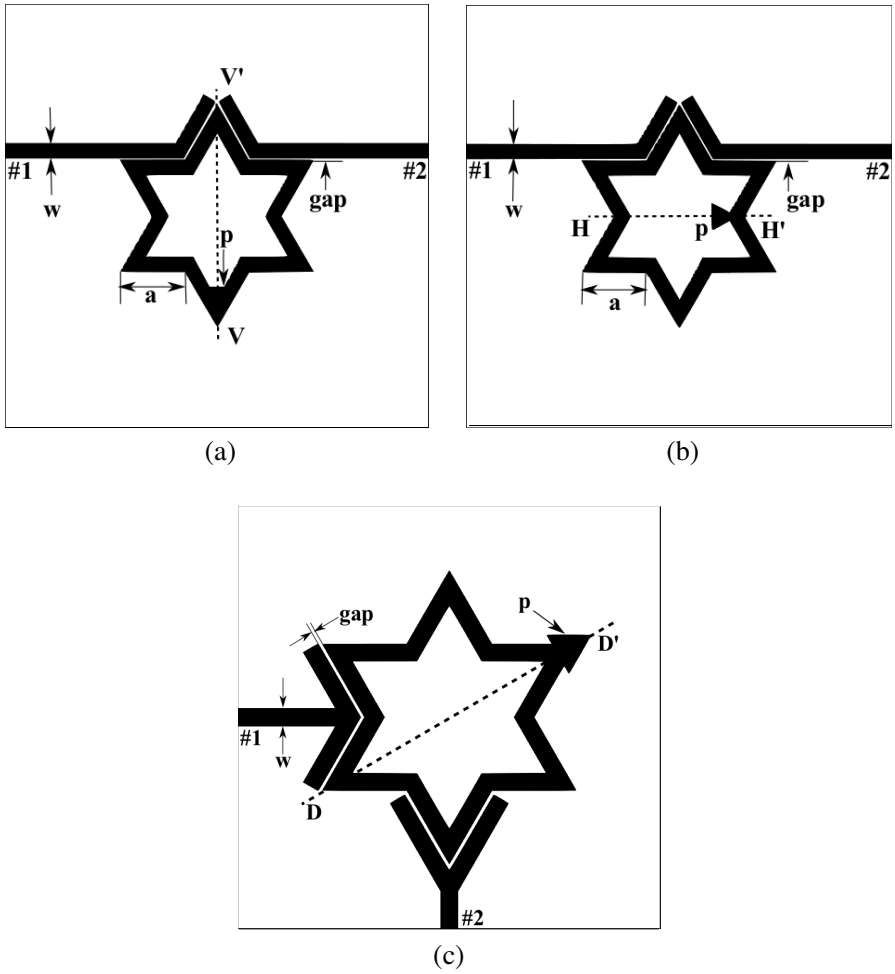

Figure 3. Dual-mode star-shaped loop bandpass filters. (a) Triangular patch placed in vertical plane (V-V'). (b) Triangular patch placed in horizontal plane (H-H'). (c) Triangular patch placed in diagonal plane (D-D').

Fig. 4(b). It is observed from Fig. 4(a) and Fig. 4(b) that location and size of the perturbation distinctively split the two modes, and the degenerated modes are represented as mode I and mode II. We can also observe that apart from the split in dual degenerate modes there is also an inherent transmission zero associated with the structure. For various perturbation sizes, only one resonant mode has varied considerably compared to the other mode. The larger the size of the perturbation is, the wider the split is in two modes. From Fig. 4(a) corresponding to the structure shown in Fig. 3(a), where the perturbation element is located in V-V' plane, the mode resonant frequency with considerable variation is named as mode II, whereas the mode which is almost constant named as mode I. These modes are validated by the simulated electric field intensity shown in Fig. 5(a) and Fig. 5(b) at 4.19 GHz and 4.27 GHz, respectively. It is seen that there are two poles in the middle of the inner bent left and right edges (H-H') and two zeros in the middle of the outer bent top and bottom edges for mode I (V-V') plane, whereas for mode II, these poles and zeros are shifted by 45 degrees in anti-clockwise direction.

Similarly, for the structure shown in Fig. 3(b), where the perturbation element is located along H-H' plane, the simulated resonant frequency variation is shown in Fig. 4(b). From Fig. 4(b), the mode with considerable variation is termed as mode I, whereas the mode with less variation is called as mode II. The electric field intensity of dual-modes for the triangular patch placed along H-H' plane is shown in Fig. 6(a) and Fig. 6(b) at 4.17 Hz and 4.11 GHz, respectively. It can be observed from Fig. 6(a) and Fig. 6(b) that for mode I, there are two zeros in H-H' plane and two poles in V-V' plane. For mode

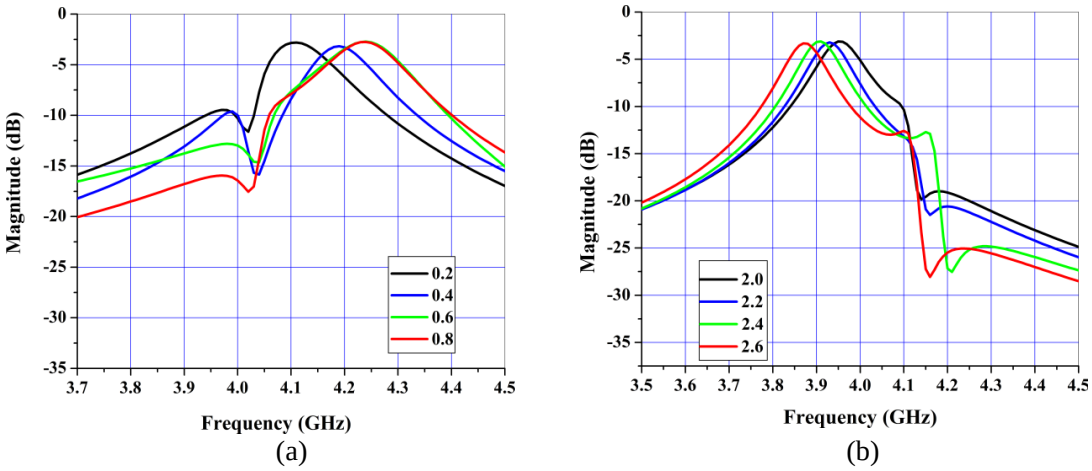

Figure 4. Frequency responses for different values of perturbation size (in mm) under weak coupling, (a) perturbation along V-V' plane and (b) perturbation along H-H' plane.

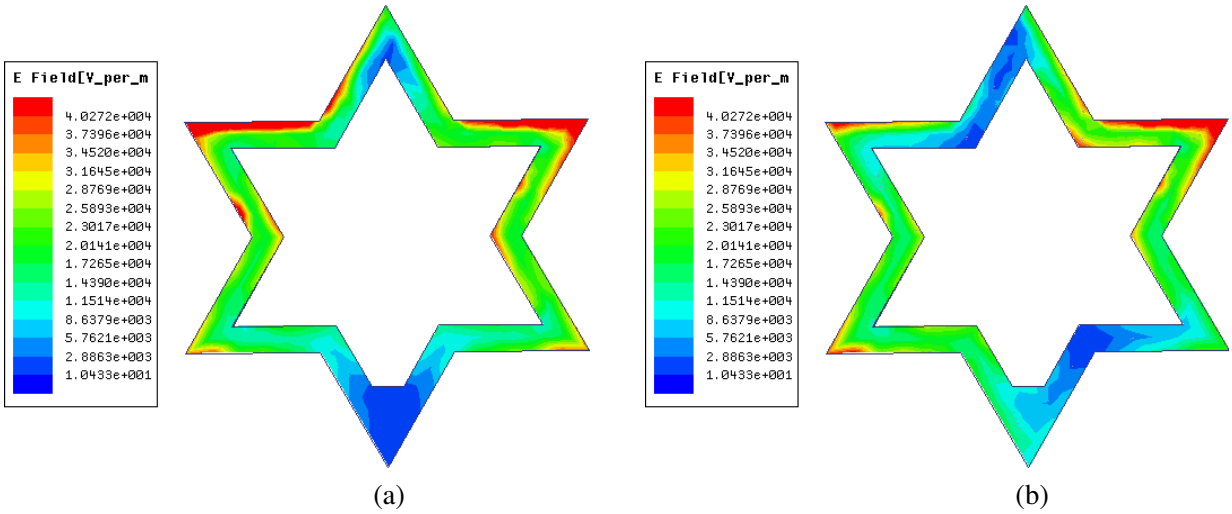

Figure 5. Simulated electric field intensity of dual modes for the triangular patch placed along V-V' plane. (a) Mode-I. (b) Mode-II.

II, they are shifted by 45 degrees in anti-clockwise direction. It is seen from Fig. 4 that there is a finite frequency transmission zero shift associated with the location and size of the perturbation element along with splitting of dual modes. As a result, transmission zero can be adjusted to appear in the lower stopband or upper stopband by using non-orthogonal feed lines and also in both sides of the passband by using orthogonal feed lines. This special property of the proposed star-shaped dual-mode resonator can be utilized for designing filters to achieve both symmetric and asymmetric frequency responses with ease.

By using HFSS eigen mode simulator, the split resonant frequencies of dual modes of a star loop resonator as a function of perturbation size 'p' are obtained, and they are plotted along with coupling coefficients as shown in Fig. 7. The coupling coefficient (K) between dual modes is calculated using Equation (1) as described in [13].

$$K = \frac{f_{02}^2 - f_{01}^2}{f_{02}^2 + f_{01}^2} \tag{1}$$

where, f_{01} and f_{02} are termed as mode-I and mode-II resonant frequencies. We can notice that in either case only one mode is varied much whereas the other mode is hardly changed. In the first case, where

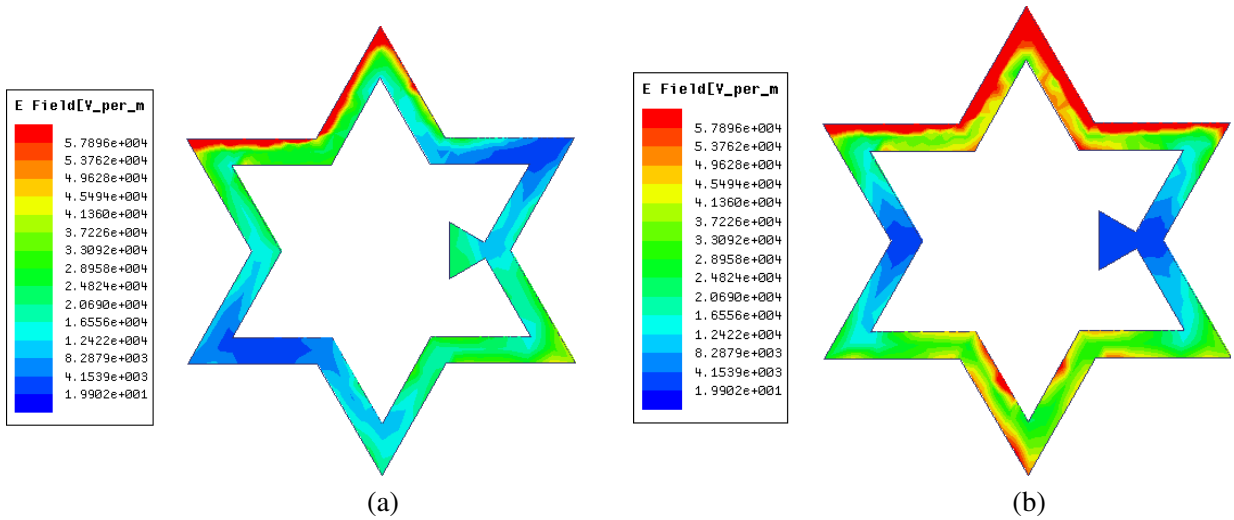

Figure 6. Simulated electric field intensity of dual modes for the triangular patch placed along H-H' plane. (a) Mode-II (4.11 GHz). (b) Mode-I (4.17 GHz).

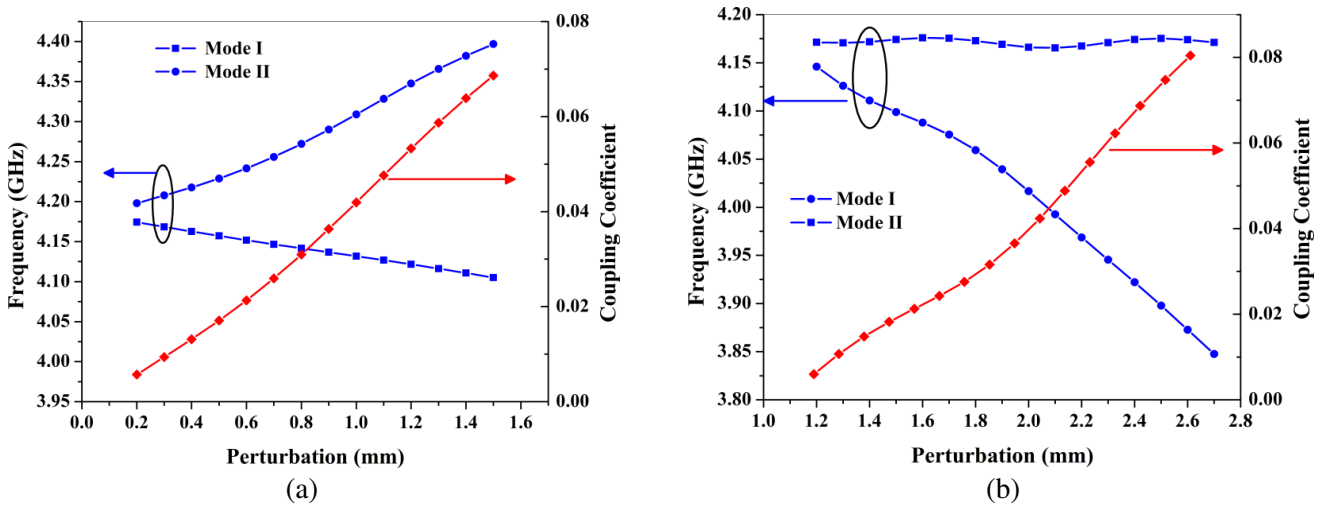

Figure 7. Simulated dual-mode resonant frequencies and coupling coefficient as a function of perturbation size, (a) perturbation element placed along V-V' plane, (b) perturbation element placed along H-H' plane.

perturbation is along V-V' plane, the frequency of mode II increases with perturbation size whereas the other mode, i.e., mode I shows little variation. When the perturbation is located along H-H' plane, the frequency of mode II is constant with respect to mode I. In either case, we can notice that there is split in the resonant frequencies and the coupling coefficient increases as the mode splitting is wider.

3. EVEN AND ODD MODE ANALYSIS

The location of transmission zeros are calculated for the proposed dual-mode star shaped resonator theoretically by using even and odd mode analysis as described in [18]. The equivalent circuit of a dual-mode filter shown in Fig. 3(a) is shown in Fig. 8(a). The even-mode half circuit is created by applying electric wall at the line of symmetry is shown in Fig. 8(b). Similarly, odd mode equivalent circuit derived by applying magnetic wall at the line of symmetry is shown in Fig. 8(c). The resultant

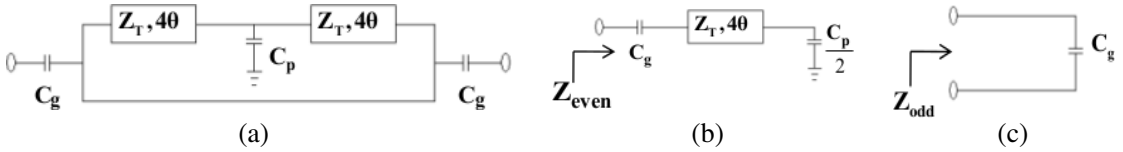

Figure 8. Equivalent circuit of (a) dual-mode filter shown in Fig. 3(a), (b) even-mode half circuit, (c) odd-mode half circuit.

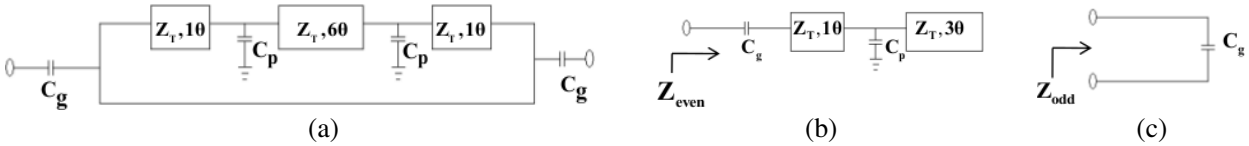

Figure 9. Equivalent circuit of (a) dual-mode filter shown in Fig. 3(b), (b) even-mode half circuit, (c) odd-mode half circuit.

even and odd mode impedances are given in Equations (2) and (3).

$$Z_{\text{even}} = -jZ_T \cot\theta + Z_{cp} + Z_{cg} \tag{2}$$

$$Z_{\text{odd}} = Z_{cg} \tag{3}$$

The location of the transmission zeros are calculated by using the condition

$$Z_{\text{even}} - Z_{\text{odd}} = 0 \tag{4}$$

Substituting Equations (2) and (3) in (4), we get the location of transmission zero frequency as

$$f_Z = \frac{f_r}{\pi} \cot^{-1}\left[\frac{-1}{2\pi f_c C_p Z_T}\right] \tag{5}$$

where, Z_T is characteristic impedance of the loop resonator. Z_{even} and Z_{odd} are the equivalent even and odd mode impedances of the half circuit. θ is the electrical length of the transmission line under consideration. f_r is the natural resonant frequency, f_c the center frequency and f_Z the transmission zero frequency. C_g and C_p denote gap and patch capacitances respectively. Under practical conditions, f_c is approximately equal to f_r. The specified values used for the calculation of transmission zero frequency are $Z_T = 50\,\Omega$ and $f_c = 4.26\,\text{GHz}$, and calculated value of patch capacitance is $C_p = 0.0393\,\text{pF}$. From Equation (5), the value of f_z is 4.18 GHz.

The equivalent circuit of dual-mode filter shown in Fig. 3(b) is shown in Fig. 9(a). The resultant even and odd mode equivalent circuit constructed by applying electric and magnetic walls at the line of symmetry is shown in Figs. 9(b) and 9(c), respectively. Even and odd mode impedances are given in Equations (6) and (7).

$$Z_{\text{even}} = \frac{\cos\theta + jy_T \sin\theta Z_{cg} + jy_T \tan 3\theta \left\{Z_{cp}\left(\cos\theta + Z_{cg}(jy_T \sin\theta)\right) + jZ_T \sin\theta + Z_{cg}\cos\theta\right\}}{jy_T \sin\theta + jy_T \tan 3\theta \left(jy_T \sin\theta Z_{cp} + \cos\theta\right)} \tag{6}$$

$$Z_{\text{odd}} = Z_{cg} \tag{7}$$

The positions of transmission zeros are calculated using the condition

$$Z_{\text{even}} - Z_{\text{odd}} = 0 \tag{8}$$

Using Equations (6) and (7) in Equation (8), we get

$$f_Z = 0.8029\frac{4f_r}{\pi} \tag{9}$$

Specified values of $Z_T = 50\,\Omega$ and $f_c = 4.13\,\text{GHz}$, and calculated value of patch capacitance is $C_p = 0.384\,\text{pF}$. The calculated transmission zero frequency using Equation (9) is 4.22 GHz.

4. DUAL-MODE BANDPASS FILTER DESIGN

Based on the above discussion, three two-pole dual-mode bandpass filters are designed, which produce both symmetrical and asymmetrical frequency response. The filters are designed using RT/Duriod substrate having a thickness of 0.635 mm, dielectric constant of 10.2 and loss tangent of 0.0023. The filters are designed and simulated using full-wave electromagnetic (EM) simulator, HFSS based on Finite Element Method (FEM). The unit length of each side of the star-shaped resonator (a) is 3 mm, and the resultant filter structure dimensions excluding feed lines are equal to 9 mm $\times$ 12 mm. The width of the feed lines and width of star loop resonator is (w) 0.59 mm, and coupling gap between resonator and feed lines is (gap) 0.2 mm. A photograph of the fabricated filters are depicted in Fig. 10. All the experimental results are measured using Agilent's N99181A series Network Analyzer.

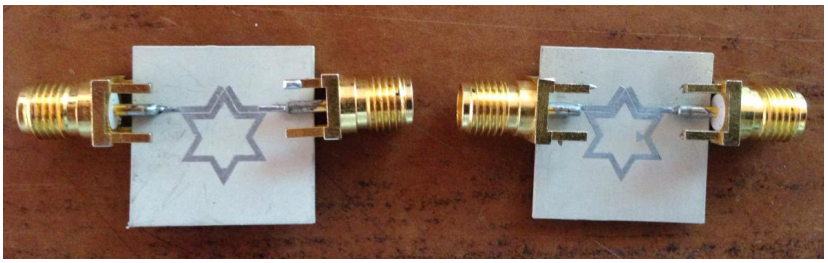

Figure 10. Photograph of the fabricated filters.

4.1. Two-Pole Asymmetric Response Dual-Mode Bandpass Filters

4.1.1. Filter with Transmission Zero in Lower Stopband

The filter layout with transmission zero in lower stopband is shown in Fig. 3(a), and it uses a pair of non-orthogonal feed lines oriented in 180 degrees straight line positioned towards the top side of the resonator. To validate the results, the corresponding filter is fabricated and shown in Fig. 10. In this structure, the triangular patch is positioned along V-V' plane which is at the bottom of the resonator, and the perturbation size is optimized to (p) 0.8 mm. The measured and simulated results are shown in Fig. 11. From Fig. 11, it has been observed that the simulated and measured results are close to each other, and the filter exhibits asymmetric response. From the measured results it is observed that

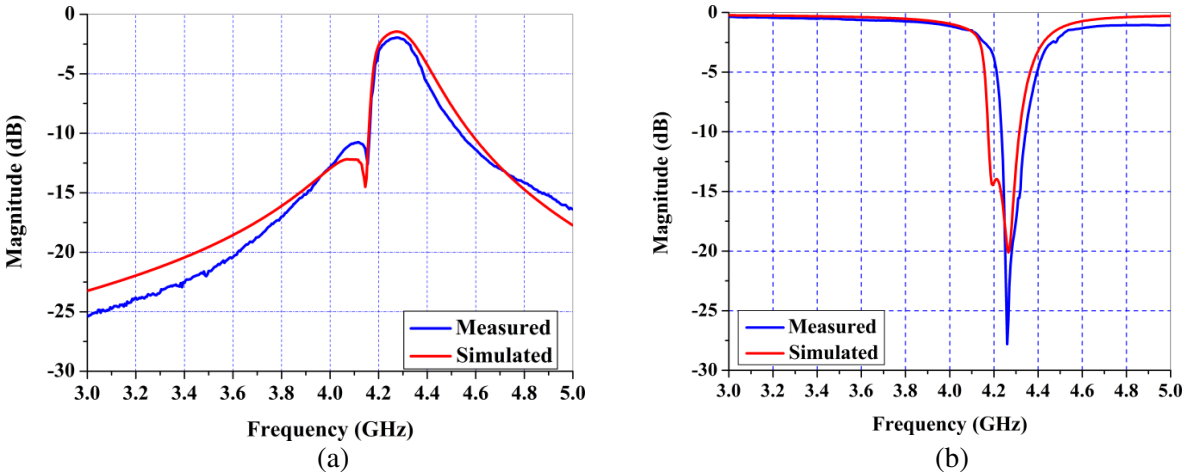

Figure 11. Simulated and measured results of the filter structure shown in Fig. 3(a), (a) insertion loss and (b) return loss.

filter is resonating at 4.26 GHz with an insertion loss of 1.97 dB and shows a peak return loss of 27 dB. The filter has a fractional bandwidth of 5.38%. The transmission zero is observed at 4.14 GHz, which is close to the calculated value of 4.18 GHz derived from Equation (5). The presence of transmission zero on the lower side of the center frequency indicates that the filter is highly selective in the lower side of the passband.

4.1.2. Filter with Transmission Zero in Upper Stopband

The layout of the filter with transmission zero in upper stopband is depicted in Fig. 3(b), and a photograph of the fabricated filter is shown in Fig. 10. The feeding mechanism adapted here is similar to the previous filter. Here triangular patch is along H-H' plane, positioned at the right side inner center of the loop. The size of the perturbation element (p) is fine-tuned to 2.5 mm to achieve an asymmetric response. Measured and simulated results of the filter are shown in Fig. 12. From the results, it is noticed that measured insertion loss of the filter is 1.78 dB at a center frequency of 4.13 GHz. The fractional bandwidth of the filter is 7.26%, and peak return loss level is at 21 dB within the passband. The transmission zero is at 4.24 GHz, which is close to the calculated value of 4.22 GHz derived from Equation (9). The presence of transmission zero on the upper side of the center frequency implies that

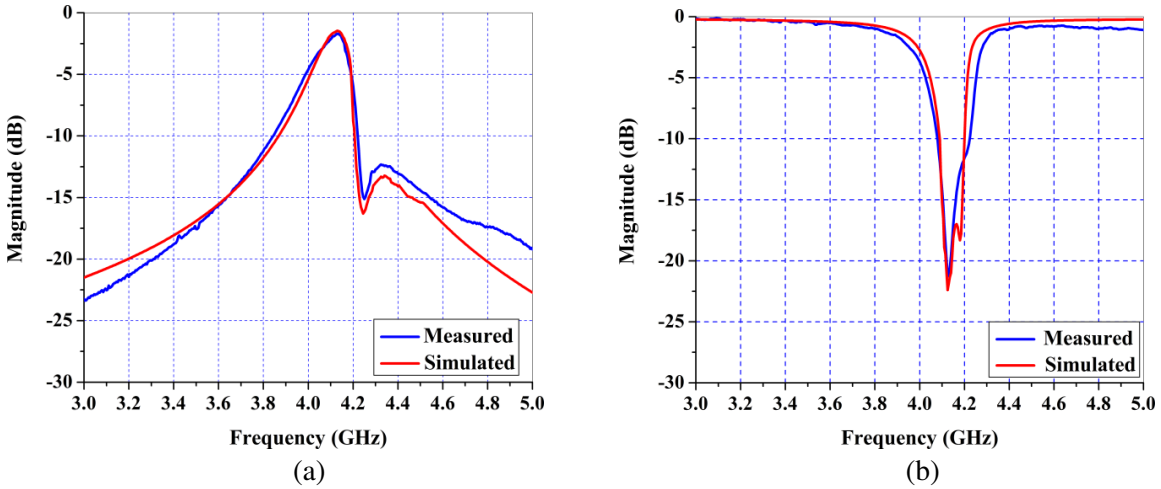

Figure 12. Simulated and measured results of the filter structure shown in Fig. 3(b), (a) insertion loss and (b) return loss.

Table 1. Comparison with previously reported dual-mode loop resonator filters.

Reference	Loop Topology	Circumference of the loop (mm)	Center frequency (GHz)	Insertion loss (dB)	FBW (%)	Size of the filter (mm × mm)	Frequency response
[12]	Square[I] Square[II]	85.6	1.86 1.9	2.06 1.92	4.4 4.4	21.4 × 21.4	Asymmetric
[5]	Triangular[I] Triangular[II]	15.5	10 10	1.4 1.4	8 8	—-	Asymmetric
[19]	Hexagonal	30.0	4.64	2.24	4.1	12.1 × 12.1	Symmetric
[20]	Octagonal Meandered	26.4	2.35	2.35	5	9.1 × 9.1	Symmetric
Proposed	Modified Star[I] Star[II]	36.0	4.26 4.13	1.97 1.78	5.38 7.26	9 × 12	Asymmetric

filter is highly selective on the upper side of the passband. The performance analysis of the filters shown in Fig. 3(a) and Fig. 3(b) is compared with other published works, and the comparison of measured results is provided in Table 1.

4.2. Two-Pole Symmetric Response Dual-Mode Bandpass Filters

The layout of the filter structure employing orthogonal feed lines to realize symmetric response is shown in Fig. 3(c). In this filter, the perturbation element is located at 135 degrees with respect to both input and output ports along D-D' plane. The triangular patch size (p) is optimized to 1.1 mm, and (gap) is 0.15 mm. Splitting of dual modes and coupling coefficient is shown in Fig. 13. The simulated electric field intensity for single-mode and dual-mode filter structures are shown in Fig. 14(a) and Fig. 14(b) at 4.10 GHz. We can observe two poles on middle right and left sides and two zeros on the top and bottom sides of the resonator for single mode structure shown in Fig. 14(a). These poles and zeros are shifted

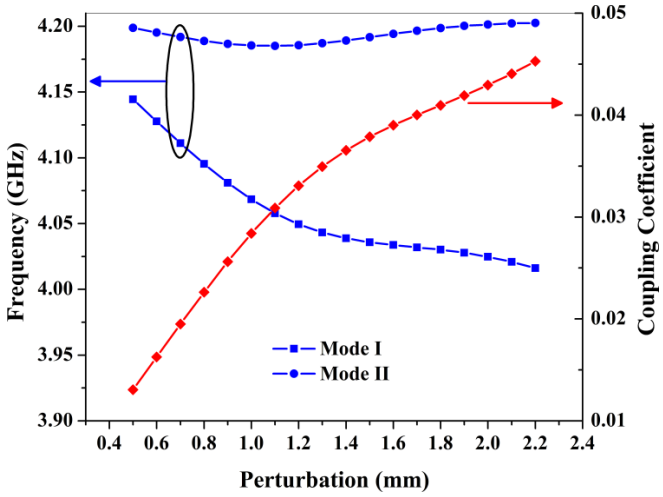

Figure 13. Simulated dual-mode resonant frequencies and coupling coefficient as a function of perturbation size placed along D-D' plane.

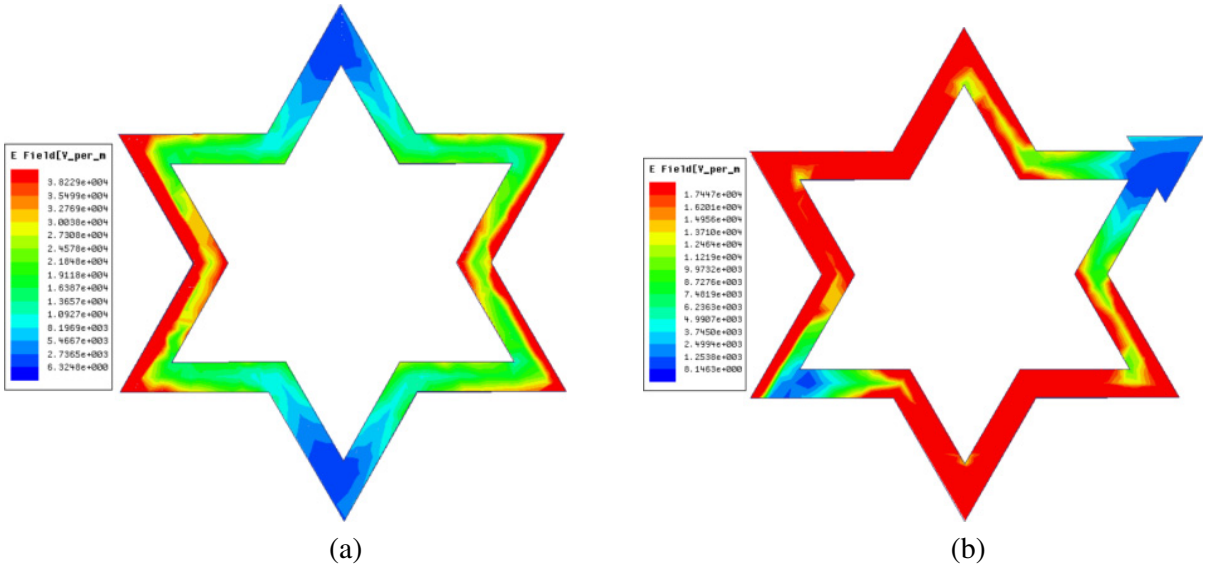

Figure 14. Simulated electric field intensity of single-mode and dual-mode star shaped resonator. (a) Single-mode. (b) Dual-mode.

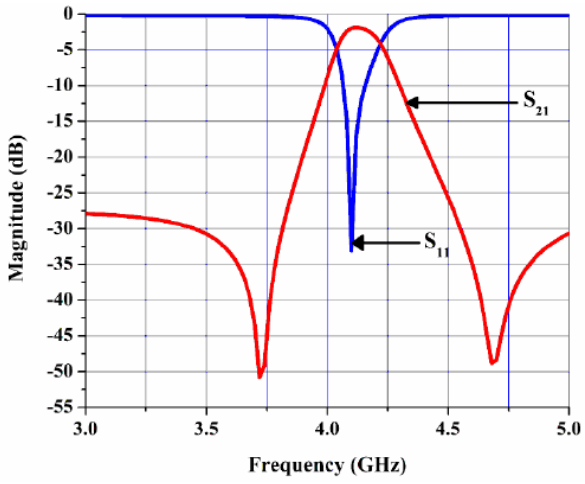

Figure 15. Simulated results of the filter structure shown in Fig. 3(c).

by 45 degrees as shown in Fig. 14(b) for dual-mode structure. The shift in the location of poles and zeros due to the perturbation element along with orthogonal feed lines generate quasi-elliptic bandpass response with two transmission zeros on both sides of the center frequency. The simulation result of the filter is demonstrated in Fig. 15, which shows an insertion loss of 2.4 dB and return loss of 32.5 dB at the center frequency of 4.12 GHz. The transmission zeros are observed at 3.7 GHz and 4.7 GHz, which validates high selectivity on both sides of the passband leading to quasi-elliptic response. It is noted that there is a slight variation in the center frequency of the three filters due to the change in size and location of the patch.

5. CONCLUSION

In this work, novel dual-mode microstrip bandpass filters using modified star-shaped loop resonator with advanced filtering characteristics are introduced. The proposed filter structures are compact and occupy a size of 9 mm × 12 mm. The distinctive characteristic of this new type of resonator is explained through EM simulations. The use of orthogonal and non-orthogonal feed lines is demonstrated. It is shown that the location and size of the triangular patch perturbation element are crucial in determining the position of transmission zeros. Even and odd mode analysis is performed to determine theoretically the location of transmission zeros. Two two-pole highly selective bandpass filters are designed, fabricated and measured. From the results it is observed that the measured and calculated transmission zero frequencies are close to each other. The first filter shows transmission zero in the lower stopband, whereas the other displays transmission zero in the upper stopband, with asymmetric frequency response. These kinds of asymmetric response bandpass filters are better suited for duplexer and multiplexer applications. Finally, a dual-mode bandpass filter with the quasi-elliptic response is presented. The designed filters have low insertion loss, good return loss with narrow fractional bandwidth. The proposed structure can also be used as a basic building block element for realizing higher order filters.

ACKNOWLEDGMENT

The authors are thankful to Bapuji Institute of Engineering & Technology, Davangere, Karnataka, India, for their kind support and encouragement towards the successful completion of this work.

REFERENCES

1. Hong, J. S. and M. J. Lancaster, *Microstrip Filters for RF/Microwave Applications*, Wiley, New York, 2001.

2. Hong, J. S. and M. J. Lancaster, "Microstrip cross-coupled trisection bandpass filters with a symmetric frequency characteristics," *IEE Proc. Microwave, Antennas Propag.*, Vol. 146, No. 1, 84–90, 1999.
3. Wolf, I., "Microstrip bandpass filter using degenerate modes of a microstrip ring resonator," *Electron. Lett.*, Vol. 8, No. 12, 302–303, 1972.
4. Hong, J. S. and M. J. Lancaster, "Bandpass characteristics of new dualmode microstrip square loop resonators," *Electron. Lett.*, Vol. 31, No. 11, 891–892, 1995.
5. Lugo, C. and J. Papapolymerou, "Bandpass filter design using a microstrip triangular loop resonator with dual-mode operation," *IEEE Microw. Wireless Compon. Lett.*, Vol. 15, No. 7, 475–477, 2005.
6. Wu, R. and S. Amari, "New triangular microstrip loop resonators forbandpass dual-mode filter applications," *IEEE MTT-S Int. Microwave Symp. Dig.*, 941–944, 2005.
7. Mansour, R. R., "Design of superconductive multiplexers using single-mode and dual-mode filters," *IEEE Trans. Microw. Theory Tech.*, Vol. 42, No. 7, 1411–1418, 1994.
8. Hong, J. S. and M. J. Lancaster, "Microstrip triangular patch resonator filters," *IEEE MTT-S Dig.*, 331–334, 2000.
9. Hong, J. S. and S. Li, "Theory and experiment of dual-mode microstriptriangular patch resonators and filters," *IEEE Trans. Microw. Theory Tech.*, Vol. 52, No. 4, 1237–1243, 2004.
10. Avinash, K. G. and I. S. Rao, "Design of bandpass filter using star loop dual mode resonator," *2015 IEEE International Conference on Communications and Signal Processing (ICCSP)*, 0238–0241, Melmaruvathur, 2015.
11. Gorur, A., "Description of coupling between degenerate modes of a dual-mode microstrip loop resonator using a novel perturbation arrangement and its dual-mode bandpass filter applications," *IEEE Trans. Microw. Theory Tech.*, Vol. 52, No. 2, 671–677, 2004.
12. Eryilmaz, G. M., C. Karpuz, and A. Gorur, "Dual-mode microstrip filters with adjustable transmission zeros," *IET Microw. Antennas Propag.*, Vol. 2, No. 8, 839–847, 2008.
13. Rouchaud, F., V. Madrangeas, M. Aubourg, P. Guillon, B. Theron, and M. Maignan, "New classes of microstrip resonators for HTS microwave filters applications," *IEEE MTT-S Dig.*, 1023–1026, 1998.
14. Hsieh, L. H. and K. Chang, "Dual-mode quasi-elliptic-function bandpass filters using ring resonators with enhanced coupling tuning stubs," *IEEE Trans. Microw. Theory Tech.*, Vol. 50, No. 5, 1340–1345, 2002.
15. Wang, J., J. L. Li, J. Ni, S. Zhao, W. Wu, and D. Fang, "Design of miniaturized microstrip dual-mode filter with source-load coupling," *IEEE Microw. Wireless Compon. Lett.*, Vol. 20, No. 6, 319–321, 2010.
16. Wang, J., J. Ni, J. B. Pan, L. Ge, and X. Y. Guo, "Design of a miniaturized microstrip dual-mode dual-band bandpass filter," *Microwave and Optical Tech. Lett.*, Vol. 53, No. 11, 1493–1496, 2011.
17. Gorur, A. K., C. Karpuz, A. Ozek, P. O. Ozdemir, and K. Karaca, "A novel compact microstrip dual-mode wideband bandpass filter design using tuning stubs," *Microwave and Optical Tech. Lett.*, Vol. 56, No. 1, 47–49, 2014.
18. Cheng, K. K. M., "Design of dual-mode ring resonators with transmission zeros," *Electron. Lett.*, Vol. 33, No. 16, 1392–1393, 1997.
19. Mao, R. J. and X. H. Tang, "Novel dual-mode bandpass filters using hexagonal resonators," *IEEE Trans. Microw. Theory Tech.*, Vol. 54, No. 9, 3526–3553, 2006.
20. Esfeh, B. K., A. Ismail, R. S. A. Raja Abdullah, H. Adam, and A. R. H. Alahwari, "Compact narrowband bandpass filter using dual-mode octagonal meandered loop resonator for WiMAX application," *Progress In Electromagnetics Research B*, Vol. 16, 277–290, 2009.